PHYSICAL REVIEW D **82,** 086006 (2010)

Anisotropic Kantowski-Sachs universe from gravitational tunneling and its observational signatures

Julian Adamek*

Institut für Theoretische Physik und Astrophysik, Julius -Maximilians-Universität Würzburg, Am Hubland, 97074 Würzburg, Germany

David Campo† and Jens C. Niemeyer‡

Institut für Astrophysik, Georg -August-Universität Göttingen, Friedrich-Hund-Platz 1, 37077 Göttingen, Germany

(Received 27 May 2010; published 8 October 2010)

In a landscape of compactifications with different numbers of macroscopic dimensions, it is possible that our Universe has nucleated from a vacuum where some of our four large dimensions were compact while other, now compact, directions were macroscopic. From our perspective, this shapeshifting can be perceived as an anisotropic background spacetime. As an example, we present a model where our Universe emerged from a tunneling event which involves the decompactification of two dimensions compactified on the two-sphere. In this case, our Universe is of the Kantowski-Sachs type and therefore homogeneous and anisotropic. We study the deviations from statistical isotropy of the cosmic microwave background induced by the anisotropic curvature, with particular attention to the anomalies. The model predicts a quadrupolar power asymmetry with the same sign and acoustic oscillations as found by the Wilkinson Microwave Anisotropy Probe. The amplitude of the effect is however too small given the current estimated bound on anisotropic curvature derived from the quadrupole.

DOI: 10.1103/PhysRevD.82.086006 PACS numbers: 11.25.Mj, 98.80.Cq, 04.62.+v

I. INTRODUCTION

If inflation lasted sufficiently long, all curvature scales imprinted on our Universe by preinflationary physics are pushed to undetectable distances beyond our current horizon. If, on the other hand, inflation ended soon after the required amount of accelerated expansion to allow a later epoch of rich structure formation in our local Universe, this cosmic amnesia may have been only partial. The largest cosmological scales observable today would then potentially show traces of the initial conditions for our inflating Universe, including curvature [1–6], anisotropies [7–9], or nontrivial topology [10]. This is the setting in which the scenario we propose can have observational consequences. While it has often been stated that fine-tuning the amount of inflation to this extent is unnatural, the landscape paradigm combined with the difficulty to find long-lasting inflationary solutions in string theory provide sufficiently strong counter arguments to take this possibility seriously [11]. Like the collision of bubbles in scenarios of false vacuum inflation (see [12] for a status report), it offers a remote chance to probe the landscape of string theory by observations.

What are plausible initial conditions for our local inflationary patch in the landscape? Compactification in string theory is often treated kinematically, as part of the construction of the effective four-dimensional theory. With four macroscopic plus a number of microscopic compact dimensions fixed once and for all, the transition between metastable vacua can be described by the spontaneous nucleation of bubbles with open homogeneous and isotropic spatial sections [13,14]. The observable consequences of false vacuum bubble nucleation followed by a brief period of slow-roll inflation have been studied extensively in the context of open inflation [2–6] and are well understood by now.

From the dynamical perspective, however, compactification becomes a problem of string cosmology, for the compactified dimensions can spontaneously open up and become large [15]. This substantially widens the parameter space for initial conditions of our local Universe, since there are now alternative channels to populate the landscape which can be viewed as transitions between vacua with differing numbers of macroscopic dimensions. This was first explicitly spelled out by Carroll, Johnson, and Randall [16] in the context of dynamical compactification from a higher dimensional spacetime to our effectively four-dimensional one. The opposite process, dynamical decompactification, was studied in [17], and in [18] in a different context.

Although these previous studies were all concerned with the (de-)compactification of higher dimensions, there is no reason to exclude that the three macroscopic dimensions of our present Universe may themselves be the result of such a process [19]. This is the starting point of our work.[1] It is

*jadamek@physik.uni-wuerzburg.de
†dcampo@astro.physik.uni-goettingen.de
‡niemeyer@astro.physik.uni-goettingen.de

[1]Shortly before completion of our work, two articles ([20,21]) were posted which have a significant amount of overlap with ours. We will comment on the similarities and differences at various places in the main text.

intuitively clear that decompactification allows the existence of a preferred direction in the sky if only one or two directions are compact, and therefore gives rise to anisotropic cosmologies. We specifically consider the case where two of our macroscopic dimensions are compact. Before inflation, these dimensions were microscopic, leaving one macroscopic direction which may still play a preferred role for cosmological observations today if inflation was short. As a concrete example, we present a four-dimensional model with two dimensions compactified on a sphere by the flux of an Abelian gauge field and a cosmological constant. The solutions of the Euclidean Einstein-Maxwell equations with spherical symmetry are well known. They describe pair creation of charged black holes in de Sitter space [22–24]. We note that the causal patch beyond the cosmological horizon in the Lorentzian spacetime is an anisotropic inflating Kantowski-Sachs (KS) universe.

This initial state can be placed in the broader context of the landscape in different ways. It can be viewed as an intermediate phase in a progressive opening up of initially compact dimensions as described in [18], or as the temporarily final step in a sequence of transitions starting from a higher dimensional geometry that triggered the decompactification of two previously compact dimensions. We comment briefly on these scenarios in Sec. II but we will leave the discussion of further implications for future work.

The remainder of this article is structured as follows. In Sec. III, the model is introduced and its connection to black hole pair production is discussed. Sec. IV presents a preliminary exploration of cosmic microwave background (CMB) signatures in our model, which are due to the anisotropy of KS spacetime. Owing to the technical complexity of a full analysis, we only consider the perturbations of a test scalar field and outline the qualitative modifications of CMB temperature anisotropies. With these results we try to assess some of the observed CMB anomalies which seem to indicate a violation of statistical isotropy in our Universe. We conclude and discuss some directions for further research along these lines in Sec. V.

II. THE SHAPESHIFTING UNIVERSE

A. Rearrangement of macroscopic dimensions

The hypothesis of a string landscape [25,26] leads to the following scenario. The effective potential of the moduli (scalar fields describing the size and shapes of compact dimensions) possesses local minima, created from the competing effects of a positive cosmological constant, the curvature of the compact spaces, fluxes, wrapped branes, etc., but also presents flat directions. The compactified configurations, which are only metastable as a consequence of gravitational tunneling, may thus open up [15,18]. Consequently, in the general case the four-dimensional macroscopic spacetime has one, two, or three compact spatial dimensions, and is anisotropic (one exceptional, and interesting case, is the compactification on a flat torus as in [27], see also [28]).

More precisely, we consider the mechanism where q dimensions are compactified on a q sphere whose radius is stabilized using the flux of an appropriate q-form field [29,30]. Many such gauge fields are available in string theories, each one coming with its own gauge coupling. One therefore obtains an entire landscape of possible flux compactifications [26]. The vacua in this landscape (the minima of the effective potential) differ in the number of large dimensions and in the effective value of their vacuum energy, which is determined by the quantum numbers of the flux fields.

These vacua are rendered metastable by the possibility to tunnel through the barriers in the effective potential of the moduli. In such a process, a bubble is formed containing a new vacuum configuration, which differs from the parent vacuum in the values of the fluxes and, possibly, in the number of compactified dimensions. Elementary transitions where compact dimensions destabilize and start to open up (decompactification), and the inverse process (compactification) have been investigated by [16,18], respectively. It has been recognized that both processes can be described with a generic type of instanton, and that the two different interpretations follow by exchanging the labels for ''parent'' and ''daughter'' vacuum. More generally, however, a vacuum transition may rearrange the configuration of compact directions in an arbitrary way, such that it is possible that some dimensions compactify while others decompactify at the same time.[2] We are thus confronted with the interesting possibility of a shapeshifting universe: some of our macroscopic dimensions may have been destabilized in the final vacuum transition which spawned our present Universe and have been opening up ever since.

The outcome of such rearrangements is that the macroscopic space dimensions have a nontrivial topology, for instance $\mathbb{R} \times \mathrm{S}_2$ corresponding to a KS spacetime, or $\mathrm{H}_2 \times \mathrm{S}_1$ corresponding to Bianchi III (BIII). Schematically, this history can be described as

$$\mathrm{dS}_D \times \mathrm{S}_2 \times \mathcal{M}_d \rightarrow \mathrm{KS}_{(4)} \times \mathcal{M}'_{d+D-2},$$

where dS_D is our effective D-dimensional parent vacuum, $\mathrm{KS}_{(4)}$ is the Kantowski-Sachs spacetime describing our macroscopic Universe, and $\mathcal{M}_d$, $\mathcal{M}'_{d+D-2}$ are additional compact manifolds. The corresponding Penrose-Carter diagram is shown in Fig. 1. Owing to the reconfiguration of the microscopic dimensions, the effective vacuum energy is changed with respect to the parent vacuum and may lie in the anthropic window if the usual conditions for the smallness of incremental changes apply [16,26].

[2]This has already been speculated in [31].

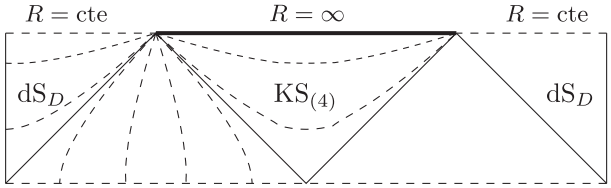

FIG. 1. Spacetime diagram of a generic tunneling process giving rise to a four-dimensional Kantowski-Sachs universe. The effective D-dimensional parent vacuum is marked as dS_D (left and right edge of the diagram should be identified). In this region, the two compact directions of our macroscopic universe approach a constant microscopic radius, as they are stabilized on S_2 by a magnetic flux. In the Kantowski-Sachs spacetime, marked as $\text{KS}_{(4)}$, these directions have destabilized and become large. Vice versa, there are $D - 2$ large dimensions in the parent vacuum which approach a compact microscopic configuration in our universe. The ''static'' regions interpolate between the parent vacuum and our bubble. The interpolation smoothly rearranges all the moduli fields to their new vacuum configuration. The case where the parent vacuum shares two large dimensions with our universe has recently been studied in [21]. In this case, the $\text{KS}_{(4)}$ region with topology $\mathbb{R} \times \text{S}_2$ is replaced by a Bianchi III spacetime, which has spatial topology $\text{H}_2 \times \text{S}_1$. The familiar result of an open FRW universe in place of $\text{KS}_{(4)}$ is obtained if all of our macroscopic dimensions are shared by our parent vacuum.

B. Description of the model

The dynamics of tunneling processes involving several interacting fields (the moduli) can be very complicated (e.g., [32]). Here, however, we are mainly interested in the geometrical properties of the corresponding instanton. Furthermore, we will treat the microscopic dimensions in our present Universe as mere spectators, and therefore we can effectively work in a four-dimensional description. The tunneling event describing the decompactification of two dimensions wrapped onto a two-sphere is then completely equivalent to the pair creation of charged black holes. It was already pointed out in [16] that the mechanism of dynamical compactification, using magnetic fluxes, is in some sense a generalization of the idea of black hole pair creation. The connection between these ways of thinking was further elucidated in [31], where different types of compactifications from a six-dimensional de Sitter vacuum have been studied.

Ignoring the additional dimensions in our description comes at the cost of not being able to represent the parent vacuum correctly, nor making quantitative statements about the tunneling rates. However, our simplified picture should accurately capture the essential geometrical properties of the daughter vacuum. In particular, within our scenario where two directions are wrapped onto a sphere, the tunneling process gives rise to a Kantowski-Sachs universe of topology $\mathbb{R} \times \text{S}_2$.

If the scales comparable to the size of the compact directions have recently entered our horizon, we may gather information about the topology of our Universe by examining, e.g., the temperature correlations in the CMB. Inflation is still a necessary ingredient in this class of models in order to dilute the spatial curvature, produce a phenomenologically viable perturbation spectrum, and heat up the Universe. However, any detection of the CMB signatures that we discuss in Sec. IV implies that inflation ended before they were redshifted too far beyond the horizon. Whether or not anthropic pressure makes this parameter range likely is an interesting debate (e.g., [11]) to which we have nothing new to add. For the purposes of this work, we simply accept it as a plausible possibility.

As the authors of [16] have shown, it is possible to accommodate a period of slow-roll inflation following the transdimensional tunneling. In their example, this is achieved by coupling an inflaton field to the curvature and flux. It was demonstrated that the tunneling process can indeed trigger slow-roll inflation by setting free the inflaton, which was previously trapped in a minimum by the configuration of the parent vacuum. In this case, the initial conditions for inflation are governed by the tunneling process. In order to simplify our analysis, we do not consider a realistic model for slow-roll inflation and absorb the inflaton potential energy into the effective cosmological constant. Thus, in our model Λ is the sum of the inflaton energy density and of the observed value of the cosmological constant.

III. KANTOWSKI-SACHS UNIVERSE FROM GRAVITATIONAL TUNNELING IN FOUR-DIMENSIONAL EINSTEIN-MAXWELL THEORY

We now introduce our cosmological model and outline the links with the pair creation of charged black holes during inflation. Most of the content of this section is well known and was originally presented in the context of black hole pair creation (see, e.g., [22–24] and references therein). In our notation and terminology, we closely follow [24].

We present our model using a unified picture where pair creation of charged black holes can equivalently be understood as Coleman-De Luccia tunneling between two different vacua of a lower dimensional effective theory. We will therefore use both interpretations interchangeably, depending on which of them is more useful in a particular situation.

As a starting point we take the action of four-dimensional Einstein-Maxwell theory,

$$\mathcal{S} = \frac{1}{16\pi} \int \mathrm{d}^4x \sqrt{-g} [\mathcal{R}[g_{\mu\nu}] - 2\Lambda - F_{\mu\nu}F^{\mu\nu}], \quad (1)$$

where a cosmological constant $\Lambda > 0$ is included in order to model inflation in a simple way. $\mathcal{R}[g_{\mu\nu}]$ is the Ricci scalar of the metric tensor $g_{\mu\nu}$, g is the metric determinant, and $F_{\mu\nu}$ is the field strength tensor of an Abelian gauge field.

We look for solutions with two of the three spatial dimensions compactified on a sphere of radius R. The line element therefore takes the form

$$\mathrm{d}s^2 = \gamma_{ab}(\mathbf{x})\mathrm{d}x^a\mathrm{d}x^b + R^2(\mathbf{x})[\mathrm{d}\theta^2 + \sin^2\theta\mathrm{d}\phi^2], \quad (2)$$

where γ_{ab} is the metric of a $1+1$-dimensional Lorentzian manifold with coordinates $\mathbf{x}$, i.e., the Latin indices take values 0 and 1 only.

The gauge field should also respect the symmetries of our metric ansatz. The magnetic solutions of Maxwell's equations are therefore proportional to the volume form of S_2,

$$\mathbf{F} = Q\sin\theta\mathrm{d}\theta\wedge\mathrm{d}\phi, \quad (3)$$

where Q is the magnetic charge.

Our next step will be the dimensional reduction of the theory by integration over the coordinates θ, ϕ of S_2. Decomposing the full Ricci scalar $\mathcal{R}[g_{\mu\nu}]$ into contributions from the S_2 curvature and from the Ricci scalar of γ_{ab}, hereafter denoted as $\mathcal{R}[\gamma_{ab}]$, the action can be rewritten as

$$S = \frac{1}{4}\int \mathrm{d}^2x\sqrt{-\gamma}\Big[R^2\mathcal{R}[\gamma_{ab}] + 2\gamma^{ab}\nabla_a R\nabla_b R + 2 - 2\Lambda R^2 - \frac{2Q^2}{R^2}\Big], \quad (4)$$

after an integration by parts has removed second derivatives on R. Variation with respect to R and γ_{ab} yields two coupled second order equations,

$$\frac{1}{2}\mathcal{R}[\gamma_{ab}]R - \Box R - \Lambda R + \frac{Q^2}{R^3} = 0, \quad (5)$$

and

$$2R\nabla_a\nabla_b R - 2\gamma_{ab}R\Box R - \gamma_{ab}\gamma^{cd}\nabla_c R\nabla_d R + \gamma_{ab}\Big(1 - \Lambda R^2 - \frac{Q^2}{R^2}\Big) = 0. \quad (6)$$

Following the usual procedure, we now solve the corresponding Euclidean equations with the boundary conditions appropriate to describe a tunneling Riemannian geometry. In Sec. III B, we consider the nucleated four-dimensional Lorentzian geometries which contain a KS spacetime. These solutions describe a universe with two compact spatial dimensions which are destabilized and start to grow.

A. Euclidean geometries

A formal analytic continuation to imaginary time takes the action to its Euclidean counterpart. The Euclidean equations remain formally identical to the Lorentzian ones (5) and (6), with the important difference that the metric γ_{ab} now has Euclidean signature $(++)$.

We consider all the solutions of the two-dimensional Euclidean equations which have $O(2)$ symmetry, meaning that all quantities only depend on the Euclidean distance χ from the symmetry point:

$$\begin{array}{rcl}\gamma_{ab}\mathrm{d}x^a\mathrm{d}x^b & = & \mathrm{d}\chi^2 + \rho^2(\chi)\mathrm{d}\varphi^2, \\ R(\chi,\varphi) & = & R(\chi).\end{array} \quad \text{(Euclidean)} \quad (7)$$

Here, the coordinate φ is an angular coordinate with period 2π. We will relate these solutions to the instantons describing pair creation of charged black holes in de Sitter space.

At the symmetry point $\chi = 0$ the Euclidean scale factor ρ is zero. The zeros of ρ are sometimes called "poles" since they may represent the origin of a polar coordinate system. In this paper, we will also call the symmetry point $\chi = 0$ the "south pole" of the geometry. If ρ has a second zero at finite $\chi = \chi_{\max}$, we will call this the "north pole." Regularity of the geometry at the poles requires $\rho'(0) = -\rho'(\chi_{\max}) = 1$, otherwise there will be a conical singularity.

Using the $O(2)$-symmetric ansatz, Eqs. (5) and (6) read, respectively,

$$\frac{\rho''}{\rho}R + R'' + \frac{\rho'}{\rho}R' + \Lambda R - \frac{Q^2}{R^3} = 0, \quad (8)$$

and

$$R'^2 + 2\frac{\rho'}{\rho}R'R - 1 + \Lambda R^2 + \frac{Q^2}{R^2} = 0. \quad (9)$$

These two equations can be combined to show that $\mathrm{d}\ln\rho = \mathrm{d}\ln R'$, which implies $\rho \propto R'$. This result can be used to eliminate ρ in Eq. (9). One finds

$$2RR'' + R'^2 - 1 + \Lambda R^2 + \frac{Q^2}{R^2} = 0, \quad (10)$$

and its first integral

$$R'^2 - \frac{Q^2}{R^2} + \frac{2M}{R} - 1 + \frac{\Lambda}{3}R^2 = 0. \quad (11)$$

These solutions are indeed the Euclidean analogs of Reissner-Nordström-de Sitter (RNdS) black holes, where the constant of integration M is the Misner-Sharp mass. The positive roots of the potential

$$V(R) \equiv -\frac{Q^2}{R^2} + \frac{2M}{R} - 1 + \frac{\Lambda}{3}R^2 \quad (12)$$

correspond to the horizons of the black hole spacetime. These are, in ascending order, the inner Cauchy horizon R_i, the black hole event horizon R_b, and the cosmological horizon R_c. There is also one root at negative R which has no physical significance.

The number of positive roots can of course be less than three. For a given Λ and a sufficiently small Q, there is a minimal and a maximal value for M at which two roots exactly coincide, such that $V(R)$ has a double root. These two situations are realized when $R_i \equiv R_b$ and $R_b \equiv R_c$, respectively. For the intermediate range of M, all three roots are distinct. This range for M shrinks as Q increases,

and at $Q = 1/\sqrt{4\Lambda}$, all three positive roots coincide for $M = 2/\sqrt{18\Lambda}$. For Q larger than that, or for M outside the intermediate range, only one positive root exists, and no instanton of finite action can be obtained. Let us first examine the cases where M is chosen such that $V(R)$ has a double root.

If R_b and R_c coincide, they designate a minimum of the potential, see Fig. 2. Hence, there is a solution $R = \text{const} = R_b(\equiv R_c)$. In this case $\rho = H^{-1}\sin H\chi$, with $H^2 = V''(R_b)/2$. [The easiest way to see this is to write $R = R_b + \delta R$ and expand Eq. (11) to second order in the perturbation δR. The functional form of ρ then follows from $\rho \propto \delta R'$, and since the amplitude of ρ is entirely fixed by the boundary conditions $\rho(0) = 0$, $\rho'(0) = 1$, it is independent of the amplitude of the perturbation.] The Euclidean solution is a sphere with radius H^{-1}. This particular solution is called the charged Nariai instanton, since the analytic continuation to Lorentzian signature turns the $S_2 \times S_2$, obtained in the full four-dimensional picture, into a $dS_2 \times S_2$ (charged) Nariai spacetime.

If, on the other hand, R_b and R_i coincide, they designate a maximum of the potential. There is again a solution $R = \text{const} = R_b(\equiv R_i)$, but this time one finds that $\rho = \omega^{-1}\sinh\omega\chi$, with $\omega^2 = -V''(R_b)/2$. The geometry is now a hyperbolic plane H_2 instead of a sphere. Since the hyperbolic plane has infinite volume, this instanton does not have a finite action. This is the reason why it is usually not discussed in the context of black hole pair creation. The spacetime one would get from analytic continuation of this instanton is $AdS_2 \times S_2$, again in the four-dimensional picture. We note that in the two-dimensional picture the compactification vacuum has negative effective vacuum energy, and hence the universe is anti-de Sitter. This seems to be a generic feature of two-dimensional vacua obtained by flux compactification. However, this does not exclude the possibility that other compactification mechanisms may give rise to effective two-dimensional solutions with positive vacuum energy. Then there would also be two-dimensional de Sitter vacua which could play the role of our parent vacuum.

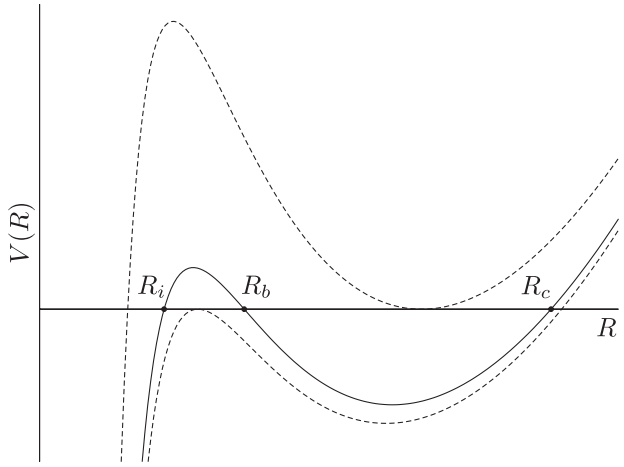

FIG. 2. Qualitative shape of the potential $V(R)$ for three different mass parameters M at fixed Λ and Q, with $Q < 3/\sqrt{48\Lambda}$. The roots of $V(R)$ correspond to the three different horizons in a Reissner-Nordström-de Sitter spacetime. The lower dashed line (smallest value of M) shows the special case when the black hole event horizon R_b and the inner Cauchy horizon R_i coincide (extremal Reissner-Nordström black hole). This potential may characterize a cold instanton as well as the $H_2 \times S_2$ instanton, which has no finite action. The upper dashed line (largest value of M) shows the special case when R_b coincides with the cosmological horizon R_c. This would be characteristic for a "charged Nariai" instanton. The line in between shows the case when $V'(R_b) = -V'(R_c)$, corresponding to a lukewarm instanton.

It is evident from Fig. 2 that in the case $R_b \equiv R_i$, a second instanton should exist. It is obtained by starting from $R = R_c$ at the south pole of the geometry. As χ increases, R rolls through the potential well and approaches $R = R_b$. However, since R_b is a double root, R reaches this value only at $\chi = \infty$. The resulting geometry is a two-dimensional $O(2)$-symmetric space which interpolates between a sphere with Gaussian curvature $V''(R_c)/2$ at the south pole and a pseudosphere with (negative) Gaussian curvature $V''(R_b)/2$ as $\chi \to \infty$. It is called the "cold" instanton, since it describes pair creation of extremal (and therefore cold) black holes. The Euclidean action of this instanton is finite and was computed, e.g., in [24].

Another special class of solutions exists when all three horizons coincide, $R_i \equiv R_b \equiv R_c$. Solutions of this type are called "ultracold". Because they are only obtained on a single point in parameter space, namely $Q = 1/\sqrt{4\Lambda}$, we do not discuss them in more detail.

Let us finally turn to the case where there are three distinct horizons. Starting again with $R = R_c$ at the south pole, one can see from Fig. 2 that now R reaches the value R_b at a finite Euclidean distance $\chi = \chi_{\max}$. Imposing the regularity condition $\rho'(0) = 1$ at the south pole, we see from Eq. (11) and $\rho \propto R'$ that a conical singularity at the north pole can only be avoided if $V'(R_c) \equiv -V'(R_b)$, which is only possible for $Q < 3/\sqrt{48\Lambda}$ and fixes the mass to $M = Q$. The instanton obtained this way is regular and has topology S_2, and its action was also computed in [24]. It describes pair creation of nonextremal charged black holes and is therefore called the "lukewarm" solution. In the terminology of [16], it corresponds to the "interpolating solution".

This completes our catalog of $O(2)$-symmetric solutions of the two-dimensional Euclidean equations. The lukewarm solutions are the only ones that we shall consider in the following, though the precise values of the parameters Q and M are not important for our discussion. We want to point out here that additional compact dimensions would not change the geometrical properties of the instanton from the two-dimensional point of view. The additional dimensions would add new moduli fields which complicate the equations, but the $O(2)$ symmetry and the

two-dimensional topology of the instanton would remain unchanged.

B. Cosmology in the spacetime of pair-created charged black holes

In the language of gravitational tunneling, the Euclidean geometries describe the solution in the classically forbidden region of configuration space. A turning-point configuration, i.e., a spacelike hypersurface which contains the initial data to solve the Cauchy problem in the classically allowed region, is given by a maximal section of the instanton, running perpendicular to the circles of constant χ from the south pole to the north pole and back again. On this surface, which has topology $S_1 \times S_2$ in the four-dimensional picture, the Euclidean solution connects to a classical Lorentzian spacetime. The $O(2)$ symmetry of the Euclidean γ_{ab} carries over to an $O(1,1)$ symmetry of the Lorentzian counterpart. Therefore, the metric solution is simply obtained by formally taking $\varphi \to it$. The line element then reads

$$\mathrm{d}s^2 = -\rho^2(\chi)\mathrm{d}t^2 + \mathrm{d}\chi^2 + R^2(\chi)[\mathrm{d}\theta^2 + \sin^2\theta \mathrm{d}\phi^2]. \quad (13)$$

Using $R'^2 = -V(R) \equiv f(R)$, $\rho \propto R'$, and absorbing the constant of proportionality into the definition of t, this can be written in the familiar form of Schwarzschild-type coordinates,

$$\mathrm{d}s^2 = -f(R)\mathrm{d}t^2 + f^{-1}(R)\mathrm{d}R^2 + R^2[\mathrm{d}\theta^2 + \sin^2\theta \mathrm{d}\phi^2]. \quad (14)$$

A causal diagram of the full classical spacetime is shown in Fig. 3.

Strictly speaking, the analytic continuation only covers the patch $R_b < R < R_c$. However, the metric (14) can simply be extended to allow $R > R_c$ or $R < R_b$, respectively, IV and II on Fig. 3, in order to cover the entire physical manifold. In these patches, R is a timelike coordinate (since $f(R)$ is negative there), and t is a spacelike coordinate, so that the metric in manifestly homogeneous (while it is static in the domain between the horizons). Furthermore, using R as a time coordinate one obtains a foliation $\mathbb{R}_{\mathrm{time}} \times (\mathbb{R} \times S_2)_{\mathrm{space}}$, which means that the two patches may be considered as two separate KS universes.

The cosmology of our own Universe is described by the KS spacetime of region IV. For a general tunneling process in the landscape of compactifications, region II will be replaced by a patch containing the parent vacuum, which may have a number of additional large dimensions, cf. Fig. 1. Regions I and V then interpolate between the parent vacuum and our own Universe. We assume that this does not drastically alter the cosmology in our Universe, though the early evolution may change somewhat as the moduli describing our microscopic dimensions settle to their new vacuum configuration.

The KS spacetime of region IV begins with a big bang which is a "pancake" singularity where only the scale factor of the noncompact direction is zero (since $R = R_c$ at this time). After a short period of curvature domination, the Universe starts to inflate. In our simple model, inflation is driven by a cosmological constant and therefore it never ends. This can be overcome by replacing Λ by an inflaton field with appropriate properties. We will assume that the initial conditions for inflation, which are determined by the tunneling process, allow for a period of slow-roll inflation in the newly nucleated universe. Explicit examples for such a scenario have been constructed in [16]. In this case, the inflaton will eventually decay and the Universe will reheat.

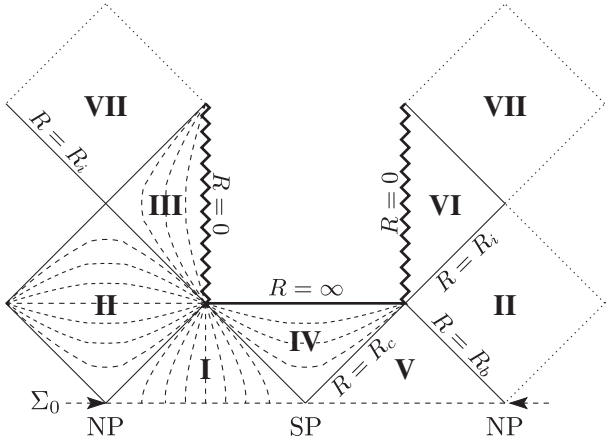

FIG. 3. Penrose-Carter diagram of Reissner-Nordström-de Sitter spacetime—left and right side (regions II and VII) should be identified. The line marked Σ_0 shows the location of the turning-point three-geometry in the diagram. It also contains the north pole and the south pole of the instanton, labeled NP and SP, respectively. Regions I and V are the static regions between the cosmological horizons and the event horizons of the two black holes. Region II is the interior of the black holes, which make up a wormhole. It is a Kantowski-Sachs universe evolving from a big bang at $R = R_b$ to a big crunch at $R = R_i$. Region IV lies beyond the cosmological horizons of the black holes. It is another Kantowski-Sachs universe which has its big bang at $R = R_c$ and starts to inflate indefinitely due to the presence of a cosmological constant. Regions III and VI lie beyond the inner Cauchy horizons $R = R_i$ and exist only in the mathematical solution, as well as region VII, which would lie in another universe. In regions I–IV, curves of constant R are sketched as dashed lines. We have omitted the time-reversed copy of the diagram below Σ_0, which would be present in a full classical solution due to time reflection symmetry. After the gravitational tunneling event has taken place, classical evolution "begins" on Σ_0.

We have presented a scenario of gravitational tunneling in which our Universe would have homogeneous but anisotropic spacelike hypersurfaces with topology $\mathbb{R} \times S_2$. In addition to this anisotropic curvature, the expansion is also anisotropic. The anisotropy of the background is reflected in observables such as the correlation of multipole coefficients in the CMB. We now present a simplified analysis of these observable signatures.

IV. OBSERVABLE SIGNATURES OF THE ANISOTROPY IN A KANTOWSKI-SACHS UNIVERSE

The nontrivial topology and geometry of the background introduces several changes with respect to Friedman-Robertson-Walker (FRW) cosmologies. First, because of the compact dimensions, the power spectrum on large scales is modified. In the event that the period of inflation was short, these scales would enter our horizon today. Second, the theory of cosmological perturbations is more intricate because scalar, vector, and tensor perturbations are coupled via the shear (see, e.g., [7,9,33] for related work in Bianchi I models). Third, the free streaming of the photons is also anisotropic, i.e., the redshift factor between the last scattering and today depends on the direction of observation (an ''anisotropic Sachs-Wolfe effect'').

These three sources of primary anisotropies cannot be treated independently in a self-consistent way because they have a common origin. We will nevertheless examine them separately by means of the following two simplifications. First, we will not present the full theory of cosmological perturbations but only examine the power spectrum of a test scalar field. Second, we disentangle the ''early'' from the ''late'' time effects, that is those resulting from the modifications of the inflationary power spectrum and the anisotropic Sachs-Wolfe effect. This is achieved by assuming that the expansion rate is isotropic after the end of inflation.

In Sec. IV A, we solve the mode equation of a massless scalar field in KS spacetime, motivate the choice of the state, and give an analytic expression of the corresponding two-point correlation function at equal time. In Sec. IV B, we project this two-point correlation function onto a sphere and calculate the corresponding multipole correlators $\langle a_{lm} a^*_{l'm'}\rangle$ for $l, l' = 2$, 3 and 4. In Sec. IV C, we discuss the additional corrections introduced by the remaining sources of anisotropies. In Sec. IV D we examine whether some of the reported CMB anomalies can be accounted for by the model.

A. Power spectrum of a massless scalar field in a Kantowski-Sachs spacetime

We begin by introducing a new set of coordinates in the inflationary KS universe of RNdS. It is important for the quantization and the definition of the ground state to work with a time coordinate which can be continued analytically beyond the cosmological horizons (into I and V of Fig. 3). The following choice satisfies this requirement:

$$\mathrm{d}s^2 = H^{-2}[-\mathrm{d}\tau^2 + V(R)\mathrm{d}z^2] + R^2[\mathrm{d}\theta^2 + \sin^2\theta \mathrm{d}\phi^2], \tag{15}$$

where we have introduced the inflationary Hubble parameter, $H \equiv \sqrt{\Lambda/3}$. In this equation, R should be read as a function of τ. Note that $V(R)$ is positive and plays the role of a scale factor for the noncompact direction z. As can be seen by comparing with Eq. (14), the spacelike coordinate is defined by $\mathrm{d}z = H\mathrm{d}t$, and the (dimensionless) time coordinate by $\mathrm{d}\tau = H\mathrm{d}R/\sqrt{V(R)}$. R is thus a growing function of τ.

Let us consider a minimally coupled massless real scalar field Φ,

$$\mathcal{S}_\Phi = -\frac{1}{2}\int \mathrm{d}^4x\sqrt{-g}g^{\mu\nu}\partial_\mu\Phi\partial_\nu\Phi. \tag{16}$$

Given a Cauchy surface of the entire spacetime such as Σ_0 on Fig. 3, Φ and its conjugate momentum are required to satisfy the canonical commutation relations. We note the Klein-Gordon product

$$(f, g) = i\int_\Sigma d\sigma^\mu\sqrt{h_\Sigma}(f^*\partial_\mu g - g\partial_\mu f^*) \tag{17}$$

and decompose the field into creation and annihilation operators $\mathrm{a}^\dagger_n$, a_n defined by

$$\mathrm{a}_n = (f_n, \Phi), \tag{18}$$

where $\{f_n\}$ is a complete family of positive norm solutions of the Klein-Gordon equation to be specified below. Following [34], we carry out this program in the following two steps. First we find the normalized solutions of the field equation in the KS wedge. Then we analytically continue the solutions beyond the cosmological horizon (into regions I and V of Fig. 3) and demand that they be regular there. This way, we avoid normalizing the solutions of the Klein-Gordon equation in regions I and V, which would require the calculation of a complicated integral.

Exploiting the $\mathbb{R}\times S_2$ symmetry of the spacelike hypersurfaces of KS, we introduce the decomposition

$$\Phi(\tau, z, \theta, \phi) = \sum_{\ell,m}\int\frac{\mathrm{d}k}{\sqrt{2\pi}}\Phi_{k\ell m}(\tau)e^{ikz}Y_{\ell m}(\theta, \phi). \tag{19}$$

We introduce the rescaled field $\Psi = |g|^{1/4}\Phi = RV^{1/4}\Phi$, in terms of which the action reads

$$S_\Psi = \frac{1}{2}\sum_{\ell,m}\int \mathrm{d}k\mathrm{d}\tau\Big\{\dot\Psi_{k\ell m}\dot\Psi^*_{k\ell m} - \Big[\frac{k^2}{V(R)} + \frac{\ell(\ell+1)}{H^2R^2} - \frac{1}{H^2} \times\Big(\frac{V'(R)}{R} - \frac{V'(R)^2}{16V(R)} + \frac{V''(R)}{4}\Big)\Big]\Psi_{k\ell m}\Psi^*_{k\ell m}\Big\}, \tag{20}$$

where we have used $\ddot R = V'(R)/2H^2$ and dropped the boundary term of an integration by parts. We further decompose the solutions into

$$\Psi_{k\ell m}(\tau) = \mathrm{a}_{k\ell m}u_{k\ell}(\tau) + (-1)^m\mathrm{a}^\dagger_{-k\ell-m}u^*_{k\ell}(\tau). \tag{21}$$

where the functions $u_{k\ell}$ satisfy the equation

$$\ddot u_{k\ell} + \Big[\frac{k^2}{V(R)} + \frac{\ell(\ell+1)}{H^2R^2} - \frac{1}{H^2}\Big(\frac{V'(R)}{R} - \frac{V'(R)^2}{16V(R)} + \frac{V''(R)}{4}\Big)\Big]u_{k\ell} = 0. \tag{22}$$

The mode functions defined by (19)–(22) form a complete family of solutions of the Klein-Gordon equation and are normalized provided

$$\mathrm{Im}\,(u_{k\ell}\dot{u}^*_{k\ell}) = 1. \tag{23}$$

The particular solution of (22) is fixed by demanding that the analytic continuation of the functions $u_{k\ell}$ to the entire spacetime is regular on a Cauchy surface, say, Σ_0 of Fig. 3 for definiteness.

In order to carry out this calculation explicitly, we make the approximation $V(R) \sim H^2R^2 - 1$. One may notice that this corresponds to work with a $\mathbb{R} \times S_2$ foliation of four-dimensional de Sitter space (see the Appendix) and one expects that it is good only if there is a separation of scales $R_c \gg R_b$, R_i. With this approximation, we have $R(\tau) = H^{-1}\cosh\tau$. We can now eliminate R from (22),

$$\ddot{u}_{k\ell}(\tau) + \left[\frac{k^2 + 1/4}{\sinh^2\tau} + \frac{\ell(\ell+1)}{\cosh^2\tau} - \frac{9}{4}\right]u_{k\ell}(\tau) = 0. \tag{24}$$

This equation can be solved exactly by substituting $s \equiv \sinh^2\tau$. The resulting equation is recognized as Riemann's differential equation whose general solution can be written in terms of the hypergeometric function ${}_2F_1$:

$$\begin{aligned} u_{k\ell} = {} & s^{1/4}s^{ik/2}\sqrt{(s+1)^{\ell+1}} \\ & \times \left[{}_2F_1\left(\frac{\ell+ik}{2}, \frac{\ell+3+ik}{2}; 1+ik; -s\right)A_{k\ell}\right. \\ & \left. + (-s)^{-ik}\,{}_2F_1\left(\frac{\ell-ik}{2}, \frac{\ell+3-ik}{2}; 1-ik; -s\right)B_{k\ell}\right] \end{aligned} \tag{25}$$

for $\ell \geq 1$. Here and in the following, we place the branch cuts such that all functions are analytic in the entire upper half of the complex plane of s, including the real line but allowing for isolated singular points. The case $\ell = 0$ has to be treated separately, the general solution in this case is

$$\begin{aligned} u_{k0} = {} & s^{1/4}s^{ik/2}\left[{}_2F_1\left(\frac{ik-1}{2}, 1+\frac{ik}{2}; 1+ik; -s\right)A_{k0}\right. \\ & \left. + (-s)^{-ik}\,{}_2F_1\left(\frac{-ik-1}{2}, 1-\frac{ik}{2}; 1-ik; -s\right)B_{k0}\right]. \end{aligned} \tag{26}$$

The constants of integration, $A_{k\ell}$ and $B_{k\ell}$, are fixed by the conditions of regularity and of normalization.[3] To implement the former, we note that we can cover the static regions of RNdS (I and V in Fig. 3) by integrating $\mathrm{d}\tau = H\mathrm{d}R/\sqrt{V(R)}$ to values $R < R_c$. The imaginary part of τ then plays the role of a radial coordinate. In a RNdS spacetime, we would impose regularity at $R = R_b$, the "north pole" of the geometry. Since we are using de Sitter space as an approximation, we instead use this condition at $R = 0$, i.e., at the poles of Euclidean de Sitter space $\tau \to \pm i\pi/2$. As seen in (24), for $\ell \geq 1$ the solutions near the poles asymptote to $u_{k\ell} \sim \rho^{\ell+1}$ or $u_{k\ell} \sim \rho^{-\ell}$, where $\tau = \pm i(\pi/2 - \rho)$. The second solution is not normalizable and is therefore excluded from the physical spectrum. Expanding the solution (25) around $s = -1$, one sees that it remains regular if the constants of integration fulfill the relation

$$B_{k\ell} = -A_{k\ell}\frac{\Gamma(1+ik)\Gamma(\frac{\ell-ik}{2})\Gamma(\frac{\ell+3-ik}{2})}{\Gamma(1-ik)\Gamma(\frac{\ell+ik}{2})\Gamma(\frac{\ell+3+ik}{2})}. \tag{27}$$

For $\ell = 0$, we impose

$$\left.\frac{\mathrm{d}u_{k0}}{\mathrm{d}R}\right|_{R=0} = 0 \tag{28}$$

such that the derivative is continuous at the poles. The constants of integration in (26) are therefore related by

$$B_{k0} = -A_{k0}\frac{\Gamma(1+ik)\Gamma(\frac{-1-ik}{2})\Gamma(1-\frac{ik}{2})}{\Gamma(1-ik)\Gamma(\frac{-1+ik}{2})\Gamma(1+\frac{ik}{2})}. \tag{29}$$

Using these relations, one can show that the normalization of the Wronskian, Eq. (23), implies

$$|A_{k\ell}|^2 = \frac{1}{k(e^{2\pi k} - 1)}, \tag{30}$$

including the case $\ell = 0$. This fixes the vacuum mode functions up to an irrelevant overall phase.

The two-point correlation function (at equal time) is finally given by

$$\begin{aligned} & \langle\Phi(\tau, 0, 0, 0)\Phi(\tau, z, \theta, 0)\rangle \\ & \quad = \sum_\ell \frac{(2\ell+1)}{16\pi^2}\int \mathrm{d}k \frac{|u_{k\ell}|^2}{R^2\sqrt{V(R)}}P_\ell(\cos\theta)e^{-ikz}, \end{aligned} \tag{31}$$

where we used homogeneity of space to shift one of the points to the origin of the coordinate system ($z = 0$, $\theta = 0$), and the rotational symmetry of S_2 to set the azimuthal coordinate ϕ of the second point to zero. We call $|u_{k\ell}|^2/R^2\sqrt{V(R)}$ the "power spectrum". It becomes time independent at late time $\tau \to \infty$,

$$\frac{|u_{k\ell}|^2}{R^2\sqrt{V(R)}} \to \frac{H^2|\Gamma(\frac{\ell+ik}{2})|^2}{2(k^2 + (\ell+1)^2)|\Gamma(\frac{\ell+1+ik}{2})|^2} \equiv \mathcal{P}_{k\ell}, \tag{32}$$

for $\ell > 0$, and

[3] In a first preprint of this paper we used a state corresponding to the solutions $\sim e^{-ik\eta}$, with $d\eta = d\tau/\sqrt{V[R(\tau)]}$ a conformal time coordinate. We see from the limiting form of Eq. (24) near the horizon, i.e., $\tau \to 0$, that they correspond to $A_{k\ell} = 0$. Some of the integrals in (40) are, however, infrared divergent for that spectrum. This infrared contribution dominated the (truncated) integrals and was responsible for a different scaling of the corrections reported there ($\propto r$ instead of $\propto r^2$). We wish to thank M. Salem for helpful correspondence concerning the appropriate definition of the vacuum state.

$$\frac{|u_{k0}|^2}{R^2\sqrt{V(R)}} \to \frac{H^2 \tanh\frac{\pi k}{2}}{k+k^3} \equiv \mathcal{P}_{k0}, \tag{33}$$

for $\ell = 0$. These results are most conveniently obtained by taking the limit $s \to \infty$ of Eqs. (25) and (26), and noting that $R^2\sqrt{V(R)} \to H^{-2}s^{3/2}$.

B. Multipole coefficients

The CMB anisotropies are described by the two-point correlation function on the two-dimensional intersection of the past light-cone of the observer with a constant time hypersurface. Anisotropic expansion during the matter dominated era causes an angular dependent redshift but for simplicity we shall neglect this additional corrections to the standard angular power spectrum in this section. Namely, we evaluate the two-point correlation function given in the previous section on a surface at fixed comoving distance and calculate the correlations between the multipole coefficients $\langle a_{lm}a^*_{l'm'}\rangle$. Our approximation amounts to assume that the post-inflationary phase of expansion is isotropic,

$$\mathrm{d}s^2 \sim -\mathrm{d}t^2 + R^2(t)[\mathrm{d}z^2 + \mathrm{d}\theta^2 + \sin^2\theta \mathrm{d}\phi^2]. \tag{34}$$

We can choose the coordinate system so that the observer is at the origin ($z = 0$, $\theta = 0$). The direction of observation $\mathbf{n}$ defines a point ($z = r\mathbf{z}\cdot\mathbf{n}$, $\theta = r\sqrt{1-(\mathbf{z}\cdot\mathbf{n})^2}$ on the last scattering surface, where $\mathbf{z}$ is the unit vector pointing along the z direction, and r is the comoving radius of the last scattering surface,

$$r = \int_{t_{\rm rec}}^{t_0} \frac{dt}{R(t)} \simeq \frac{3.5}{\dot{R}(t_0)} = 3.5\sqrt{\Omega_{\rm curv}}, \tag{35}$$

see the Appendix for the definitions. We also record the relation between the ratio r and the number of e-folds of inflation. Since the shear is small, the radius of the last scattering surface is in the first approximation equal to its value in isotropic cosmologies $l_{\rm LSS} \simeq 0.5H_0^{-1}$. Let us define the origin of the number of e-folds as the instant where the radius of the compact directions R is of the order of the Hubble radius today $H_0^{-1} \simeq R$. If inflation lasts $N_{\rm extra} > 0$ additional e-folds, this radius is $e^{N_{\rm extra}}$ larger. Hence,

$$r = \frac{l_{\rm LSS}}{R} \simeq 0.5e^{-N_{\rm extra}}. \tag{36}$$

A long period of inflation therefore corresponds to $r \ll 1$.

The correlations between the multipole coefficients are given by

$$\langle a_{lm}a^*_{l'm'}\rangle = \int \mathrm{d}\Omega \mathrm{d}\Omega' Y_{lm}(\mathbf{n}) Y^*_{l'm'}(\mathbf{n}') \langle \Phi(\mathbf{n}, r)\Phi(\mathbf{n}', r)\rangle. \tag{37}$$

Before we start to calculate, we note that some of them vanish by invariance under point-reflection, which is a symmetry of the KS model. The two-point function in the above expression is indeed even under parity and the correlations between multipole coefficients of opposite parity, i.e., such that $l + l'$ is odd, vanish identically. Parity is also a symmetry of the Bianchi III models considered in [20,21], which explains why they also find no correlations for the multipole coefficients where $l + l'$ is odd.

We now introduce intrinsic spherical coordinates (ϑ, φ) on the last scattering surface. For simplicity, we choose the polar axis aligned with the z direction such that $\mathbf{z}\cdot\mathbf{n} = \cos\vartheta$. As we have already seen in the previous section, homogeneity of space guarantees that the two-point function in the above equation only depends on two parameters: the separation along the flat direction z, given by $r(\cos\vartheta - \cos\vartheta')$, and the angle θ subtended by an arc on the compact dimensions, that is $\cos\theta = \cos(r\sin\vartheta)\cos(r\sin\vartheta') + \sin(r\sin\vartheta)\sin(r\sin\vartheta')\cos(\varphi - \varphi')$, as some simple geometric considerations show. In order to simplify our expressions, we will use the identity

$$P_\ell(\cos\theta) = \frac{4\pi}{2\ell+1}\sum_{n=-\ell}^{\ell} Y^*_{\ell n}(r\sin\vartheta, \varphi) Y_{\ell n}(r\sin\vartheta', \varphi'). \tag{38}$$

Using Eq. (31), the multipole correlations in terms of these intrinsic coordinates become

$$\langle a_{lm}a^*_{l'm'}\rangle = \int \mathrm{d}\Omega \mathrm{d}\Omega' \sum_\ell \int \mathrm{d}k Y_{lm}(\vartheta, \varphi) Y^*_{l'm'}(\vartheta', \varphi') \frac{\mathcal{P}_{kl}}{4\pi} \times \sum_{n=-\ell}^{\ell} Y^*_{\ell n}(r\sin\vartheta, \varphi) Y_{\ell n}(r\sin\vartheta', \varphi') e^{-ikr(\cos\vartheta - \cos\vartheta')}. \tag{39}$$

Since KS spacetime is axially symmetric around the z axis, and since our choice of intrinsic coordinates respects that symmetry, the coefficients a_{lm} with different m are uncorrelated. One can show this explicitly by integrating out the angles φ and φ',

$$\langle a_{lm}a^*_{l'm'}\rangle = \delta_{mm'}\sqrt{2l+1}\sqrt{2l'+1}\sqrt{\frac{(l-m)!}{(l+m)!}\frac{(l'-m)!}{(l'+m)!}}\int_0^\pi \sin\vartheta \mathrm{d}\vartheta \int_0^\pi \sin\vartheta' \mathrm{d}\vartheta' \int \mathrm{d}k P_{lm}(\cos\vartheta) P_{l'm}(\cos\vartheta') \times \sum_\ell \mathcal{P}_{kl}\frac{2\ell+1}{16\pi}\frac{(\ell-m)!}{(\ell+m)!} P_{\ell m}(\cos(r\sin\vartheta)) P_{\ell m}(\cos(r\sin\vartheta')) e^{-ikr(\cos\vartheta - \cos\vartheta')}. \tag{40}$$

TABLE I. Relative deviations from a flat Friedman-Robertson-Walker cosmology of the multipole correlations. The numerical results are for $r = 0.5$. Solid convergence was achieved for the leading digit only. We found that for the nonzero entries $\delta C_{ll'mm'}$ is roughly proportional to r^2, cf. Fig. 4.

$\delta C_{ll'mm}$	$m = 0$	$m = 1$	$m = 2$	$m = 3$
$l = 2, l' = 2$	+0.02(40)	+0.01(16)	−0.02(48)	-
$l = 2, l' = 3$	0	0	0	-
$l = 2, l' = 4$	−0.005(4)	−0.005(0)	−0.003(3)	-
$l = 3, l' = 3$	+0.02(29)	+0.01(62)	−0.00(04)	−0.02(69)
$l = 3, l' = 4$	0	0	0	0

We calculate the remaining coefficients $\langle a_{lm} a^*_{l'm'} \rangle$ numerically. We compare these results with the statistically isotropic case of a flat FRW universe with a Harrison-Zel'dovich spectrum

$$\langle a_{lm} a^*_{l'm'} \rangle_{\rm iso} = \frac{H^2}{2\pi} \frac{1}{l(l+1)} \delta_{ll'} \delta_{mm'}. \tag{41}$$

This expression is obtained by computing the vacuum expectation value in the Bunch-Davies vacuum using the flat slicing of de Sitter space.

We present our results in the following form:

$$\langle a_{lm} a^*_{l'm'} \rangle = \frac{H^2}{2\pi} \delta_{mm'} (\delta_{ll'} + \delta C_{ll'mm}) \times \max\left\{ \frac{1}{l(l+1)}, \frac{1}{l'(l'+1)} \right\}, \tag{42}$$

and give the coefficients $\delta C_{ll'mm}$ in Table I for the case $r = 0.5$, which corresponds to $\Omega_{\rm curv} \simeq 0.02$, see Eq. (35). The scaling of the coefficients $\delta C_{ll'mm}$ with r is illustrated in Fig. 4. Our findings are the following. First, the amplitude of the corrections is suppressed by $r^2 \propto \Omega_{\rm curv}$. In the limit of a long period of inflation, $r \to 0$, i.e., when the observer only has access to scales much smaller than the radius of S_2, the anisotropies become unobservable. Second, as already pointed out the correlations vanish by parity for $l + l'$ odd. This result does not depend on our choice of coordinate system. Third, the amplitude of the corrections is largest for $l = l'$, and generally decreases with growing $|l - l'|$. It is also noteworthy that the amplitude, at fixed $|l - l'|$, is almost independent of l, which means that the correlations extend uniformly up to arbitrarily high multipoles. Fourth, for $l = l'$, the m dependence of the corrections obeys

$$\delta C_{llmm} = \delta C_{ll00} \left(1 - \frac{3m^2}{l(l+1)} \right) \tag{43}$$

to a good approximation. As a result, the corrections cancel in the averaged multipole

$$C_l \equiv \sum_m \frac{\langle a_{lm} a^*_{lm} \rangle}{2l+1} = \frac{H^2}{2\pi} \frac{1}{l(l+1)}. \tag{44}$$

Fifth, from Eq. (35) we deduce

$$\delta C_{ll00} \simeq \Omega_{\rm curv}. \tag{45}$$

A mild dependence on l of the prefactor is possible.

We emphasize two remarkable properties of these spectra. The first one is the scale invariance of the power spectrum, and, in particular, the absence of an infrared cutoff which one could have naively expected from the asymptotic form of the power spectrum (32) and (33) at $k \to 0$ or by analogy with closed FRW models. The second is the fact that, as we already pointed out, at a given value of l, the anisotropy manifests itself by a redistribution of the power amongst the various a_{lm} according to the "sum rule"

$$\sum_m \delta C_{llmm} = 0. \tag{46}$$

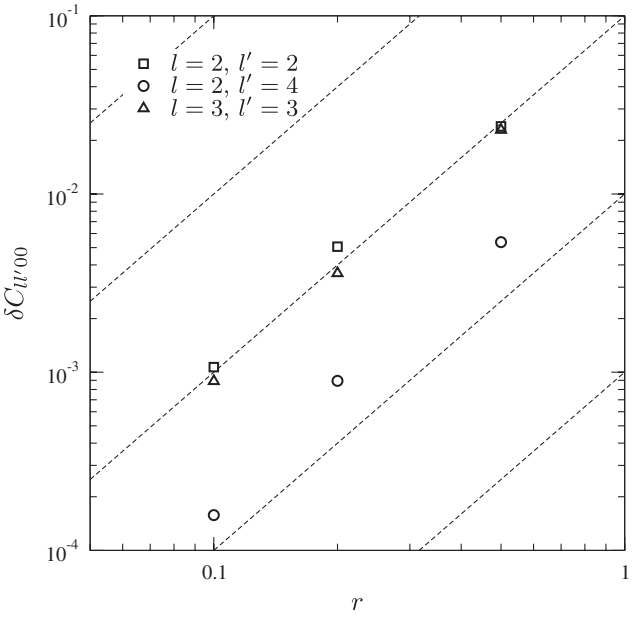

FIG. 4. Amplitude of the anisotropic correction to the multipole correlators for different values of r (three examples). We found a scaling consistent with $\delta C_{ll'mm'} \propto r^2$, as indicated by the dashed lines.

In Sec. IV D, we show how Eqs. (43) and (46) translate into observables (the so-called bipolar coefficients). Eqs. (43)–(46) and Table I are the central results of this section.[4]

In [21], a table similar to our Table I can be found for a Bianchi III model. The deviations due to anisotropy are controlled in that case by the comoving radius of the last scattering surface, $\rho_\star$ in their notation, and scale like $\rho_\star^2 \propto \Omega_{\rm curv}$. Their table and ours are remarkably similar,[5] the only difference appears to be the overall sign of the corrections. It is tempting to conjecture that this is related to the opposite sign of the curvature of Bianchi III models as compared to KS models. Note as well that Eq. (43) then should hold for both cases, as seems to be implied also by Fig. 3 of [21]. The resulting cancellation of the corrections when taking the sum over m was, however, not reported in [21].

C. Corrections to the Sachs-Wolfe effect

Our analysis of anisotropic signatures was simplified in two respects. First, we only consider a test field. Without a detailed analysis, it is hard to determine whether the theory of cosmological perturbations in KS spacetime would give primordial spectra qualitatively different from the ones of perturbed FRW spacetimes, besides the ones already found for test scalar fields. We leave this question for future work. Our second simplification is that we neglected the anisotropic redshift after last scattering. In a KS spacetime, this effect is controlled by the ratio of the shear, δ, to the isotropic expansion rate H (see the Appendix for the definitions). This ratio decreases during inflation but grows again during radiation and matter domination, so that it becomes significant only at small redshifts $z = \mathcal{O}(1)$. These late-time effects are thus determined by the value of the ratio

$$\sigma = \frac{\delta_0}{H_0}. \tag{47}$$

To get a handle on the additional corrections brought by the anisotropic redshift of photons since last scattering, note that this effect has two origins in our model. One is caused by the anisotropic expansion and the second by the curvature of the homogeneous surfaces. To see the effect of the anisotropic expansion alone, consider a Bianchi I model $ds^2_{\rm BI} = -dt^2 + a^2(t)dx^2 + b^2(t)(dy^2 + dz^2)$. The null geodesic equation is readily solved and gives the temperature distribution in the direction (ϑ, φ)

$$T_{\rm BI}(\vartheta, \varphi, t_O) = T_{\rm em}\left(\frac{x^2}{a^2_{\rm em}} + \frac{y^2 + z^2}{b^2_{\rm em}}\right)^{-1/2}, \tag{48}$$

where $T_{\rm em}$ is the temperature of the Planck spectrum at the time of emission, and the Cartesian coordinates (x, y, z) are related to the intrinsic coordinates on the unit sphere by $x = \sin\vartheta\cos\varphi$, $y = \sin\vartheta\sin\varphi$, and $z = \cos\vartheta$. The quadrupole character of this distribution is obvious (recall that when written in Cartesian coordinates, the spherical harmonics of weight l are homogeneous polynomials of degree l). We conclude that the anisotropic Sachs-Wolfe effect takes the form

$$\left(\frac{\delta T}{T}\right)_{\rm BI} \sim \frac{\Psi}{3}\left(1 + \sum_{m=-2}^{m=2} \mathcal{O}(\sigma) Y_{2m}(\vartheta, \varphi)\right) + \ldots \tag{49}$$

where Ψ is the gravitational potential in the Newtonian gauge and the ellipsis stands for the corrections from the velocity potential of matter and the integrated Sachs-Wolfe term, both of which receive similar quadrupolar *modulations*. Inserted into the expression (37) of the correlation functions, this quadrupole generates additional correlations between the $\langle a_{lm} a^*_{l'm'}\rangle$ with $l' = l, l \pm 2$.

The non Euclidean character of the surface of homogeneity in KS spacetimes is responsible for additional corrections to the geodesic equation. As a result, the temperature distribution cannot be written in closed form as in the simple expression (48). Nevertheless, inspection of the geodesic equations is sufficient to show that these corrections scale with σ as one could expect. Indeed, the null component of the momentum is given by

$$\frac{dp_0}{d\lambda} = \delta\left\{-2e^{4\Delta}\bar{p}_z^2 + e^{-2\Delta}\left(\bar{p}_\theta^2 + \frac{\bar{p}_\phi^2}{\sin^2\theta}\right)\right\} \tag{50}$$

where $\Delta = \int^t \delta$ and $\bar{p}_{z,\theta,\varphi}$ are integration constants.

A detailed calculation of the bolometric flux, which includes all of these corrections, was done in [20] for Bianchi III spacetimes. It can easily be adapted to the Kantowski-Sachs spacetime and confirms the qualitative results we have just derived. Moreover, it is noteworthy that the diagonal corrections δC_{llmm} retain the same parametric form (43) and therefore verify the sum rule (46), as can be seen from Eq. (47) of [20], with the use of their equations (B1) and (B3). Since we expect that both early and late modifications of the power spectra add at leading order in $\Omega_{\rm curv}$, the total correction should therefore also verify Eqs. (43) and (46).

[4]We also note that because of the sum rule (46), the corrections to the (cosmic) variance of the estimator $\hat{C}_l \equiv \sum_m |a^{\rm obs}_{lm}|^2/(2l + 1)$ are only quadratic in $\Omega_{\rm curv}$. Indeed with use of Eq. (43) one obtains

$$\mathrm{Var}[\hat{C}_l] = \frac{2C_l^2}{2l+1}\left[1 + \frac{1}{5}\left(4 - \frac{3}{l(l+1)}\right)\delta C^2_{ll00}\right],$$

where it is still assumed that the field is Gaussian.

[5]It is worth pointing out that their calculations differ significantly from ours. While we calculated the integrals (40) numerically, the authors of [21] made a series of approximations to simplify the corresponding expression [their Eq. (4.33)] before resorting to numerics. The agreement between our results and theirs, where they overlap, gives a good indication that these approximations, rather hard to justify rigorously, are correct.

D. CMB anomalies

We now ask whether the correlations of the multipole coefficients we have computed in the previous sections can account for some of the anomalies found in the CMB (see [35,36] for recent reviews and references). We can, in fact, discuss both KS and BIII models because they have important features in common and therefore make very similar predictions. Moreover, although we have not calculated explicitly the corrections from the recent history of the Universe, we saw that the parametric form Eq. (43) holds for both, and therefore for the total correction of the CMB spectra.

Here we make no statement regarding either the cold spots, which would require an analysis far beyond the scope of this paper, or the alignment of the dipole and quadrupole with the ecliptic, which is unlikely to have a cosmological explanation.

Also, from the scale invariance of the primordial power spectrum, and, in particular, the absence of a cutoff (see Eq. (44)) we conclude that the KS and BIII models seem unable to explain the lack of power at large scales (of the quadrupole and of the correlation function) and the disparity between odd and even values of l. However, the quadrupole receives a nonstochastic contribution in anisotropic models which, in a complete calculation, may have a number of different sources (see Sec. IV D 1 for further details.)

The KS and BIII models can, however, in principle account for the alignment of the quadrupole and octopole and the quadrupolar power asymmetry. A statistical analysis reveals that the effect of anisotropy on the alignment is not significant. On the other hand, we find good indications that the quadrupolar asymmetry can be explained by the KS model, but not by BIII. However, as we now explain the amount of anisotropic curvature needed to produce a signal with the observed amplitude, $\Omega_{\rm curv} \simeq 10^{-2}$, is probably inconsistent with the nondetection of a CMB quadrupole at the same level.

1. The quadrupole moment and the bound on curvature

In anisotropic models, the late-time expansion couples multipoles l and $l+2$ [20]. The quadrupole thus receives a *nonstochastic* contribution from the monopole proportional to $T_0\Omega_{\rm curv}$. Given a model with a scale invariant power spectrum of amplitude $\delta T/T_0 \sim 10^{-5}$, and in the absence of other sources of quadrupolar anisotropy, the value of anisotropic curvature is thus expected to be [37]

$$\Omega_{\rm curv} \lesssim 10^{-4}. \tag{51}$$

For the purpose of model building we note that, through the relationships (35) and (36), it implies a lower bound on the duration of inflation, $N_{\rm extra} \gtrsim 2.7$. Moreover, we will see that this bound, if correct, is too stringent for the model to account for the quadrupolar asymmetry in the CMB.

It is, however, important to stress that this bound is a rough estimate obtained under the assumption of adiabatic perturbations [37]. A detailed calculation might show this estimate to be too naive, since compensations might occur between the Doppler, proper Sachs-Wolfe and integrated Sachs-Wolfe terms in a KS and BIII universe, as is the case in, e.g., open inflation scenarios [38,39]. Moreover, a mixture of adiabatic and isocurvature perturbations presumably also modifies the bound (51). Thus one must bear in mind that Eq. (51) depends on the details of the model and might be too stringent.

2. Alignment of the quadrupole and octopole

We study the problem of the alignment with the help of the so-called multipole vectors [40]. The two quadrupole vectors define a plane whose normal $\mathbf{v}$ is obtained by taking the cross-product of the two vectors. Similarly, all possible pairings of the three octopole vectors define three different planes, with normals $\mathbf{w}^{(1)}$, $\mathbf{w}^{(2)}$, $\mathbf{w}^{(3)}$. One says that the octopole is planar when the three $\mathbf{w}^{(i)}$ are almost collinear, and one says that the quadrupole and octopole are aligned when they are also almost collinear with $\mathbf{v}$.

The degree of alignment is measured by the statistics

$$S \equiv \frac{1}{3}\sum_i |\mathbf{v}\cdot\mathbf{w}^{(i)}| \tag{52}$$

A large value of S indicates an alignment. The observed value (taken from the Doppler-corrected internal linear combination map, WMAP seven-year data, see [41]) is $S_{\rm ILC7} = 0.736$.[6]

For a Gaussian and statistically isotropic distribution of a_{lm} we found that only about 1% of the realizations have a value of S larger than $S_{\rm ILC7}$. According to [35], this ''remarkable degree of alignment'' lacks a compelling theoretical explanation. Unfortunately, we will now show that the class of KS and BIII models do not provide one.

For each model and each set of parameters, we generated 10^6 independent realizations of a quadrupole and octopole. To this end, the coefficients a_{lm} are treated as independent (remember that the correlations between quadrupole and octopole vanish) Gaussian random variables with zero mean[7] and variance $\langle a_{lm}a^*_{lm}\rangle$ given in Eq. (42). For each

[6]In order to be able to compare our results with others, we followed the general practice where the vectors $\mathbf{v}$ and $\mathbf{w}^{(i)}$ are *not* normalized. The use of normalized vectors instead affects the significance level by an order of magnitude. It was argued that the effective weighting introduced by non normalized vectors accounts for ''how well'' the plane is defined by the two vectors of the cross product, a badly defined plane being one where the angle between these vectors is small (since the norm of the vector is proportional to the sine of this angle) [36]. This position is untenable, because a plane is geometrically defined by two noncollinear vectors. Hopefully, the bias introduced by the weighting is less important for the relative statistical significance, i.e., when comparing two models, than it is for the absolute statistical significance, i.e., for a given model.

[7]Since the late-time expansion in anisotropic models couples multipoles l and $l+2$ [20], the quadrupole receives a nonstochastic contribution from the monopole proportional to $T_0\Omega_{\rm curv}$. We limit however our analysis to whether the correlations of the primordial spectrum can themselves favor an alignment.

realization, we calculate the corresponding multipole vectors from the coefficients a_{lm} using the algorithm of [42], and compute from them the value of S. We set $\delta C_{3300} \simeq \delta C_{2200}$, as indicated from our Table I, and with the use of (43) we then study how the distribution of S varies as a function of the single parameter $\delta C_{2200} \simeq \Omega_{\rm curv}$.

For both KS and BIII spacetimes (that is for either sign of δC_{2200}), the mean of the distribution shifts towards larger values, indicating a tendency of the quadrupole and octopole to align. However, the distribution of S turns out to be fairly robust. In particular, the mean value and variance of S change very little. For instance, in KS the mean value of S increases by only $\sim 1\%$ for $\delta C_{2200} \simeq 0.4$. The effect is about twice as large for BIII. The skewness depends more strongly on δC_{2200}, and, in particular, on its sign. It increases for $\delta C_{2200} < 0$ (BIII) and decreases for $\delta C_{2200} > 0$ (KS). For $\delta C_{2200} \simeq \pm 0.2$ the skewness changes by $\sim 20\%$ in both cases. As a result of the increase of both the mean and skewness, the number of realizations which exceed the threshold $S_{\rm ILC7}$ in BIII is increased by $\sim(5\%, 18\%, 62\%)$ for $\delta C_{2200} \simeq (-0.1, -0.2, -0.4)$, while it hardly changes for KS. The number of realizations nevertheless remains of the same order of magnitude as in the isotropic case.

In conclusion, we find that the modified multipole correlations in KS and BIII are unable to account for the alignment of the quadrupole and octopole at a statistically significant level.

3. Quadrupolar power asymmetry

A practical way to check whether the two-point correlation function $\mathcal{C}(\mathbf{n}, \mathbf{n}')$ is invariant under rotation is to consider its representation in the basis of the total angular momentum operator of eigenvalues L and M (sometimes referred to as bipolar spherical harmonics [43]). Using the ''bra-ket'' notation, we have

$$\langle \mathbf{n}, \mathbf{n}' | \mathcal{C} \rangle = \sum_{l,l',L,M} N^L_{ll'} A^{LM}_{ll'} \langle \mathbf{n}, \mathbf{n}' | ll'; LM \rangle, \tag{53}$$

where we follow the normalization convention chosen by the WMAP team [35] in order to facilitate comparison:

$$N^L_{ll'} \equiv \sqrt{\frac{(2l+1)(2l'+1)}{2L+1}} \langle l, 0, l', 0 | ll'; L0 \rangle. \tag{54}$$

The $A^{LM}_{ll'}$ are the sum over m and m' of the $\langle a_{lm} a^*_{l'm'} \rangle$ weighted by the appropriate Clebsch-Gordan coefficients. Since the eigenstates $|ll'; LM\rangle$ generate a $(2L+1)$-dimensional representation of the rotation group, the condition that $\mathcal{C}$ is statistically isotropic reads

$$\begin{aligned} &\mathcal{C}(\mathcal{R}\mathbf{n}, \mathcal{R}\mathbf{n}') = \mathcal{C}(\mathbf{n}, \mathbf{n}') \quad \forall\ \mathcal{R} \in SO(3) \\ &\Leftrightarrow A^{LM}_{ll'} = 0 \quad \forall\ L > 0, \end{aligned} \tag{55}$$

where $\mathcal{R}$ is an arbitrary rotation. If some of the $A^{LM}_{ll'}$ are nonzero for $L = 1$, the CMB temperature presents a dipole modulation. If some coefficients are nonzero for $L = 2$, the temperature is modulated by a quadrupole as, for example, we found for the late-time effects Eq. (49) (see the appendix of [35] for other illustrations).

Note that the $A^{LM}_{ll'}$ are in general not independent of the choice of a coordinate system. The WMAP team uses a preferred coordinate system in which all coefficients with $M \neq 0$ are consistent with zero. In KS spacetime this coincides with the coordinate system we use in our calculations.

With the use of Eq. (43) we find that $A^{00}_{ll} = C_l$ and

$$A^{20}_{ll} = \frac{C_l}{\sqrt{5}} \left(4 - \frac{3}{l(l+1)} \right) \delta C_{ll00}. \tag{56}$$

There is no dipole modulation because of the parity symmetry of the background which entails vanishing correlations for $l' = l \pm 1$. The important remark concerning (56) is that these coefficients are proportional to C_l. Therefore they should exhibit acoustic oscillations as well.

The WMAP team found that $A^{20}_{ll} \approx -2A^{20}_{l-2,l}$. As illustrated in the appendix of [35], this relation occurs when the anisotropy does not induce any correction to the average power spectrum but only redistributes the power amongst the a_{lm}. So we expect to find it in our model. Having calculated the correlations only up to $l = 4$, we can only check the relation for that value. From our Table I we obtain $A^{20}_{24} \simeq -0.001 \times H^2/(2\pi)$. With $\delta C_{4400} \simeq \delta C_{3300}$ we find indeed that $A^{20}_{44} \approx -2A^{20}_{24}$.

In conclusion, the anisotropy in the KS and BIII models shows all of the characteristic features found in the WMAP data. In particular, the appearance of the acoustic peak in the A^{20}_{ll} naturally follows from such models. The predictions of the models however differ in the *sign* of the bipolar coefficients A^{20}_{ll} which is determined by the sign of the curvature. We find that KS predicts the correct sign.

Unfortunately, if the bound on anisotropic curvature (51) is correct, the predicted amplitude is 2 orders of magnitude too small. Indeed, from Fig. 16 of [35], we get $A^{20}_{ll}/C_l \simeq 4 \times 10^{-2}$, which according to expression (56) corresponds to δC_{ll00}, and therefore $\Omega_{\rm curv}$, of the order of a few percents. However, as we recalled in Sec. IV D 1 the anisotropic curvature has another effect: it adds a nonstochastic component to the quadrupole of the order of $T_0 \Omega_{\rm curv}$ [20,37], which leads to the bound $\Omega_{\rm curv} \lesssim 10^{-4}$. With a value of the anisotropic curvature in that range, the quadrupolar anisotropy cannot be accounted for by the model.

V. SUMMARY AND CONCLUSIONS

In the landscape of string theory, vacua with differing numbers of macroscopic dimensions and topologies are connected by tunneling events. In this paradigm, our Universe has been produced as the last step in a potentially long chain of events, by tunneling from a parent vacuum with a greater, equal, or smaller number of macroscopic

dimensions. Like [20,21] which appeared when our work was near completion, we consider the latter case. Our approach differs in the specific model under examination and in its embedding into a cosmological scenario, which we dubbed the ''shapeshifting universe.'' Specifically, we take the example of a spacetime where two of our current macroscopic dimensions are compactified on a two-sphere by a magnetic flux.

The existence of a long-lived parent vacuum with two macroscopic dimensions, while all others are stably compactified, is not a necessary requirement for this scenario. All we need is a precursor with two of our four large dimensions compactified while other, currently compact, directions may well have been macroscopic. This allows a direct connection of anisotropic cosmologies produced by decompactification with the vast possibilities of transdimensional vacuum transitions described in [16,31] and, furthermore, admits histories with greatly varying effective values of Λ. In one particular possible scenario, our parent vacuum was a $\mathrm{dS}_D \times \mathrm{S}_2$ spacetime with higher Λ_{eff} and different compact directions than our Universe, connected to ours by a combined spontaneous compactification of $D-2$ dimensions which are now small and decompactification of the S_2. We have not explicitly constructed the instanton describing this shapeshifting event but we know of no reasons why it should not exist. It is also plausible that models can be constructed where inflation is triggered by the transition, as described in [16].

This line of investigation raises a number of new and interesting questions. In the context of the cosmological measure problem, the contribution of regions with different numbers of macroscopic dimensions and transitions in between is still largely unexplored (see [16,21,31] for some ideas). We hope to return to this question in future work. From the phenomenological point of view, on the other hand, decompactification offers a concrete framework for parameter studies of anisotropic cosmological models. Our ability to detect statistical anisotropy hinges on the assumption of a sufficiently short period of inflation, which again may find some justification in the string theory landscape. Given the observational constraints, a small but nonzero window for anisotropic curvature remains (see, e.g., [20]). Precisely how strong the constraints already are, and how much can be gained by combining future large-scale galaxy surveys and CMB data, can only be answered by a more detailed investigation of the cosmological signatures of models like the one proposed here. It is also interesting to note that having embedded the anisotropic universe model in a more complete scenario of quantum tunneling, where the KS spacetime corresponds to only a wedge of a large spacetime, solves the ambiguity in the ground state (compare with the discussions of [7,9]).

Our preliminary analysis of the deviations from statistical isotropy of the CMB shows the following trends. Some of the off-diagonal correlations $\langle a_{lm} a^*_{l'm'} \rangle$, which vanish in the isotropic case, are now nonzero. Because of the invariance under point-reflection of the background, the correlations with l and l' of different parities vanish. The nonzero correlations receive contributions from both the inflationary phase and the recent expansion of the Universe. Both scale as Ω_{curv} in the observations. The central results are the Table I and the Eqs. (43) and (46). We showed that as a direct consequence of this, and in contrast to Bianchi III models, the Kantowski-Sachs models predict a quadrupolar modulation in the CMB with all the features observed in the data, namely, the sign of the bipolar coefficients $A^{LM}_{ll'}$, their acoustic oscillations, and a particular relation between them. To obtain the observed amplitude requires, however, an anisotropic curvature at a level of $\Omega_{\mathrm{curv}} \simeq 10^{-2}$, which is incompatible with the bound derived from the value of the quadrupole, namely $\Omega_{\mathrm{curv}} \lesssim 10^{-4}$. We briefly argued that this bound could be mitigated. The price to pay is unfortunately an increased complexity of the model, which we leave for future work. We conclude that the model in its present, most simple, form is unable to account for any of the anomalies.

As an additional line for future investigation we mention the generation of primordial magnetic fields. Since KS spacetimes are not conformally flat, we indeed expect that long wavelength magnetic fields are produced from vacuum fluctuations during inflation, without recourse to noncanonical couplings of masses. This generation could perhaps be sufficient to explain the primordial magnetic fields necessary to seed galactic dynamos.

ACKNOWLEDGMENTS

We thank M. Salem and M. Johnson for valuable comments on the first preprint of this article. J. C. N. would also like to thank R. Bousso, B. Freivogel, R. Harnik, M. Johnson, A. Lewis, and I-S. Yang for helpful discussions, and acknowledges the hospitality of the Berkeley Center for Theoretical Physics and the Aspen Center for Physics where many of them took place. We further wish to thank the anonymous referee for useful comments and A. Rakić for some insights on the CMB anomalies. The work of J. A. was supported by the German Research Foundation (DFG) through the Research Training Group 1147 ''Theoretical Astrophysics and Particle Physics.''

APPENDIX: KANTOWSKI-SACHS SPACETIMES

A. Geometry

We collect some useful properties of KS spacetimes [44]. They are (locally) homogeneous, that is they are invariant under an isometry group G which acts transitively on the spacelike hypersurfaces (i.e., for two points x and y, there exists an isometry $g \in G$ such that $g \circ x = y$). The group has four parameters and admits a three-parameter subgroup isomorphic to $SO(3)$. The Killing vectors therefore verify the Lie algebra $[X_i, X_j] = \epsilon_{ijk} X_k$ with

$i = 1, 2, 3$ and $[X_4, X_i] = 0$. Moreover there exists locally a coordinate system (t, z, θ, ϕ) which diagonalizes the metric,

$$ds^2 = -dt^2 + a^2(t)dz^2 + b^2(t)(d\theta^2 + \sin^2\theta d\phi^2), \quad \text{(A1)}$$

where z is the coordinate of the flat direction, and (θ, ϕ) are the intrinsic coordinates on a two-sphere. Then $X_4 = \partial/\partial z$ and X_i are the familiar generators of the rotation group. Because of the spherical symmetry, and since it is not conformally flat, KS is of Petrov type D. The principal null directions are in the plane (t, z).

It is good to make a pause here and compare with the perhaps better known Bianchi classes. Bianchi classes I, V, VII, and IX have a universal covering with constant spatial curvature. Bianchi class I is probably the most studied anisotropic space to date because it has locally Euclidean spatial sections [7–9,45]. Classes II, IV, and VIII do not have an obvious cosmological application. Finally, class III resembles closest KS spacetimes. The spatial metric is

$$ds^2_{\mathrm{BIII}} = -dt^2 + a^2(t)dz^2 + b^2(t)(d\chi^2 + \sinh^2\chi d\phi^2). \quad \text{(A2)}$$

Like in KS spacetime, the orbits are two-dimensional. At first sight, the only difference between KS and BIII is the sign of the curvature, the topology of the spacelike hypersurfaces of BIII being $\mathbb{R} \times \mathrm{H}_2$. But the metric is deceptive for one can show that the isometry group of BIII admits a second three-parameter subgroup whose orbits are three dimensional, which is not the case if the two-dimensional orbits have a positive curvature (see in particular [46] for details). In that sense, BIII and KS spacetimes form two distinct classes. Note finally that BIII spaces can be compactified by identifying points on the spacelike surfaces with respect to a discrete subgroup of G, yielding a multiconnected space, for instance a torus [47].

B. Evolution

Returning to KS spacetimes, the spatial sections are described by the Ricci scalar ${}^3\mathcal{R} = 1/b^2$ and the intrinsic curvature tensor is $K^i{}_j = \frac{1}{2}h^{ik}\partial_t h_{kj} = \mathrm{diag}(\alpha, \beta, \beta\sin^2\theta)$, with $\alpha = \dot{a}/a$ and $\beta = \dot{b}/b$. Its trace, the local expansion rate in the frame (A1), is $K = \gamma^{ij}K_{ij} = \alpha + 2\beta$. The shear, $\sigma^i{}_j = K^i{}_j - \delta^i{}_j K/3 = \frac{1}{3}\mathrm{diag}(-2\delta, \delta, \delta)$ with $\delta = \beta - \alpha$, characterizes the anisotropy of the expansion. Einstein's equations with a perfect fluid are

$$2\alpha\beta + \beta^2 + \frac{1}{b^2} = T_{tt} = \rho \quad \text{(A3)}$$

$$2\frac{\ddot{b}}{b} + \beta^2 + \frac{1}{b^2} = -T_{zz} = -p_z \quad \text{(A4)}$$

$$\frac{\ddot{a}}{a} + \frac{\ddot{b}}{b} + \alpha\beta = -T_{\theta\theta} = -T_{\phi\phi} = -p_\theta \quad \text{(A5)}$$

and the Bianchi identities are

$$\dot{\rho} + K\rho + \alpha p_z + 2\beta p_\theta = 0. \quad \text{(A6)}$$

We can combine the first three equations to obtain equations for the local expansion rate and shear

$$\frac{1}{3}(K^2 - \delta^2) + \frac{1}{b^2} = \rho, \quad \text{(A7)}$$

$$\dot{K} + \frac{K^2}{3} + \frac{2}{3}\delta^2 = -\frac{1}{2}(\rho + P), \quad \text{(A8)}$$

$$\dot{\delta} + K\delta + \frac{1}{b^2} = 0, \quad \text{(A9)}$$

where we note $P = p_z + 2p_\theta$.

The autonomous system formed by these equations has been analyzed in [48] and the possible singularities were described. Assuming the equation of state $p_i \simeq -\rho$, the case relevant for our inflationary model is a pancake singularity, i.e., $a \to 0$ and $b \to$ cte for $t \to -\infty$, where only the noncompact direction grows in the first stage dominated by curvature. The physical variables behave as ${}^3\mathcal{R} \sim K^2/3 \sim \delta^2/3 \sim \rho$. Once inflation starts, the curvature term $1/b^2$ in Eq. (A7) becomes negligible and the universe becomes effectively isotropic and asymptotes to de Sitter space, $a \sim b \sim e^{Ht}$. To see this, use (A7) to eliminate δ^2 from (A8) and write $K = 3\dot{\Omega}/\Omega$ to get $\ddot{\Omega}/\Omega = 2\rho/3 \simeq$ cte. Hence, $K \simeq \mathrm{cte} = 3H$ and $\Omega \simeq \Omega_0 \cosh(H(t - t_0))$. Finally, substitution of this solution in (A9) or (A7) gives $\delta \propto e^{-2Ht}$. In view of this solution, it is reasonable to expect that inflation is an attractor solution as in isotropic cosmologies.

The asymptotic behavior translates as follows in the coordinate system (14). For large enough R, $f(R) \simeq 1 - \Lambda R^2/3$ becomes a good approximation and (14) coincides with the static de Sitter metric

$$\mathrm{d}s^2 = -(1 - H^2R^2)\mathrm{d}t_s^2 + (1 - H^2R^2)^{-1}\mathrm{d}R^2 + R^2[\mathrm{d}\theta^2 + \sin^2\theta\mathrm{d}\phi^2], \quad \text{(A10)}$$

de Sitter space indeed admits a foliation $\mathbb{R} \times \mathrm{S}_2$ obtained simply by extending (A10) to the region where R is timelike, $R > R_c \equiv H^{-1}$, followed by an obvious change of coordinates which puts then the metric in the form

$$\mathrm{d}s^2 = -\mathrm{d}t^2 + \frac{\sinh^2 Ht}{H^2}\mathrm{d}z^2 + \frac{\cosh^2 Ht}{H^2}(\mathrm{d}\theta^2 + \sin^2\theta\mathrm{d}\phi^2). \quad \text{(A11)}$$

Cosmological models based on de Sitter space are usually studied in foliations of a Friedman-Robertson-Walker type, i.e., which are both homogeneous and isotropic, either closed, open, or flat. This choice is not available in the spacetime of black hole pairs because symmetry dictates that homogeneous fields are functions of R, and therefore homogeneous slices are slices of constant R.

From the previous results, we can assume that reheating is an isotropic process, and therefore the CMB is such that $p_z = p_\theta = \rho/3$. The equation of conservation of the energy (A6) is then solved trivially $\rho \propto \Omega^{-4}$. From Stefan's law we get that a surface of constant temperature is

$$T = \text{cte} \Leftrightarrow \Omega = \text{cte} \Leftrightarrow t = \text{cte} \tag{A12}$$

Since $\delta \ll 1$, Eqs. (A7) and (A8) with the terms δ^2 neglected are the familiar Friedman equations. For an equation of state $p = (\gamma - 1)\rho$, we thus get in the first approximation $a \sim b \sim t^{2/3\gamma}$. The general solution of Eq. (A9) is

$$\delta = \delta_0\left(\frac{\Omega_0}{\Omega}\right)^3 + \frac{1}{ab^2}\int_{t_0}^{t} dt' a(t') \sim \frac{3\gamma}{3\gamma+2} t^{1-4/3\gamma}. \tag{A13}$$

The last approximation is obtained after substituting the solutions of a and b previously found and noticing that the homogeneous solution is subleading. We could then use (A13) to iterate an asymptotic expansion for a, b and δ. Thus during matter domination, the ratio of the shear to the isotropic expansion rate grows like

$$\frac{\delta}{H} \sim t^{2/3} \sim \Omega. \tag{A14}$$

This can be re-expressed in terms of the curvature parameter defined by

$$\Omega_{\text{curv}} = \frac{1}{b^2 H^2} \sim t^{2/3}. \tag{A15}$$

The relation with the parameter r of Eq. (35) follows from their respective definitions: $r = l_{\text{LSS}}/R$ is the radius of the last scattering surface in the units of the radius of S_2, and $\Omega_{\text{curv}} = (l_{H_0}/R)^2$ is the square of the Hubble length in those units. The relation (35) follows from the proportionality of l_{LSS} and l_{H_0}.

We note finally that these results are readily adapted to the Bianchi type III since only the sign of the curvature term $1/b^2$ changes. By contrast in Bianchi I, where the spatial hypersurfaces are Euclidean, only the first term on the right-hand side of (A13) is present, and (A14) is replaced by $\delta/K \sim \Omega^{-3/2}$.

[1] B. Freivogel, M. Kleban, M. Rodríguez Martínez, and L. Susskind, J. High Energy Phys. 3 (2006) 039.
[2] K. Yamamoto, M. Sasaki, and T. Tanaka, Astrophys. J. **455**, 412 (1995).
[3] K. Yamamoto, M. Sasaki, and T. Tanaka, Phys. Rev. D **54**, 5031 (1996).
[4] J. García-Bellido and A. R. Liddle, Phys. Rev. D **55**, 4603 (1997).
[5] A. Linde, M. Sasaki, and T. Tanaka, Phys. Rev. D **59**, 123522 (1999).
[6] J. García-Bellido, J. Garriga, and X. Montes, Phys. Rev. D **60**, 083501 (1999).
[7] A. E. Gümrükçüoğlu, C. R. Contaldi, and M. Peloso, J. Cosmol. Astropart. Phys. 11 (2007) 005.
[8] T. S. Pereira, C. Pitrou, and J.-P. Uzan, J. Cosmol. Astropart. Phys. 09 (2007) 006.
[9] C. Pitrou, T. S. Pereira, and J.-P. Uzan, J. Cosmol. Astropart. Phys. 04 (2008) 004.
[10] M. Lachieze-Rey and J.-P. Luminet, Phys. Rep. **254**, 135 (1995).
[11] A. De Simone and M. P. Salem, Phys. Rev. D **81**, 083527 (2010).
[12] A. Aguirre and M. C. Johnson, arXiv:0908.4105.
[13] S. R. Coleman and F. De Luccia, Phys. Rev. D **21**, 3305 (1980).
[14] A. Aguirre and M. C. Johnson, Phys. Rev. D **73**, 123529 (2006).
[15] S. B. Giddings, Phys. Rev. D **68**, 026006 (2003).
[16] S. M. Carroll, M. C. Johnson, and L. Randall, J. High Energy Phys. 11 (2009) 094.
[17] J. J. Blanco-Pillado, D. Schwartz-Perlov, and A. Vilenkin, J. Cosmol. Astropart. Phys. 12 (2009) 006.
[18] S. B. Giddings and R. C. Myers, Phys. Rev. D **70**, 046005 (2004).
[19] R. H. Brandenberger and C. Vafa, Nucl. Phys. **B316**, 391 (1989).
[20] P. W. Graham, R. Harnik, and S. Rajendran, arXiv:1003.0236 [Phys. Rev. D (to be published)].
[21] J. J. Blanco-Pillado and M. P. Salem, J. Cosmol. Astropart. Phys. 07 (2010) 007.
[22] R. Bousso and S. W. Hawking, Phys. Rev. D **54**, 6312 (1996).
[23] R. Bousso and S. W. Hawking, Int. J. Theor. Phys. **38**, 1227 (1999).
[24] R. B. Mann and S. F. Ross, Phys. Rev. D **52**, 2254 (1995).
[25] L. Susskind, arXiv:hep-th/0302219.
[26] R. Bousso and J. Polchinski, J. High Energy Phys. 06 (2000) 006.
[27] H. Ooguri, C. Vafa, and E. P. Verlinde, Lett. Math. Phys. **74**, 311 (2005).
[28] B. McInnes, Nucl. Phys. **782**, 1 (2007).
[29] M. Grana, Phys. Rep. **423**, 91 (2006).
[30] C. Krishnan, S. Paban, and M. Žanić, J. High Energy Phys. 05 (2005) 045.
[31] J. J. Blanco-Pillado, D. Schwartz-Perlov, and A. Vilenkin, J. Cosmol. Astropart. Phys. 05 (2010) 005.
[32] M. C. Johnson and M. Larfors, Phys. Rev. D **78**, 083534 (2008).
[33] M.-a. Watanabe, S. Kanno, and J. Soda, arXiv:1003.0056.

[34] M. Sasaki, T. Tanaka, and K. Yamamoto, Phys. Rev. D **51**, 2979 (1995).
[35] C. L. Bennett *et al.*, arXiv:1001.4758.
[36] C. J. Copi, D. Huterer, D. J. Schwarz, and G. D. Starkman, arXiv:1004.5602.
[37] M. Demiaski and A. G. Doroshkevich, Phys. Rev. D **75**, 123517 (2007).
[38] J. Garcia-Bellido, A. R. Liddle, D. H. Lyth, and D. Wands, Phys. Rev. D **52**, 6750 (1995).
[39] D. Langlois, Phys. Rev. D **55**, 7389 (1997).
[40] C. J. Copi, D. Huterer, and G. D. Starkman, Phys. Rev. D **70**, 043515 (2004).
[41] D. Sarkar, D. Huterer, C. J. Copi, G. D. Starkman, and D. J. Schwarz, arXiv:1004.3784.
[42] J. R. Weeks, arXiv:astro-ph/0412231.
[43] A. Hajian and T. Souradeep, Astrophys. J. **597**, L5 (2003).
[44] R. Kantowski and R. K. Sachs, J. Math. Phys. (N.Y.) **7**, 443 (1966).
[45] T. R. Dulaney and M. I. Gresham, Phys. Rev. D **81**, 103532 (2010).
[46] C. B. Collins, J. Math. Phys. (N.Y.) **18**, 2116 (1977).
[47] H. V. Fagundes, Phys. Rev. Lett. **51**, 517 (1983).
[48] E. Weber, J. Math. Phys. (N.Y.) **25**, 3279 (1984).